



## Heterogeneous solar photo-Fenton treatment of industrial wastewater via $\delta$ -FeOOH

K E Barrera-Salgado<sup>1</sup>, C A Pineda-Arellano<sup>2</sup>, A Álvarez-Gallegos<sup>3</sup>, J Hernández-Pérez<sup>3</sup> & S Silva-Martínez\*,<sup>3</sup>

<sup>1</sup>Posgrado en Ingeniería y Ciencias Aplicadas de la FCQeI-CIICAp, Universidad Autónoma del Estado de Morelos.  
Av. Universidad 1001, Col. Chamilpa, Cuernavaca, Mor. C.P. 62209, México

<sup>2</sup>Conacyt- Centro de Investigaciones en Óptica A.C. Prol. Constitución 607, Fracc. Reserva Loma Bonita.  
Aguascalientes, Aguascalientes, México. Código Postal 20200.

<sup>3</sup>Centro de Investigaciones en Ingeniería y Ciencias Aplicadas. Universidad Autónoma del Estado de Morelos,  
Av. Universidad 1001, Col. Chamilpa, Cuernavaca, Mor. C.P. 62209, México.

E-mail: [ssilva@uaem.mx](mailto:ssilva@uaem.mx)

Received 14 November 2019; accepted 17 September 2020

The wastewater from the textile industry has been treated with heterogeneous solar photo-Fenton using iron oxyhydroxides ( $\delta$ -FeOOH and FeOOH) nanoparticles.  $\delta$ -FeOOH and FeOOH catalysts have been prepared, respectively, from ferrous and ferric ions as precursor species using an easy and low-cost method. The FeOOH catalyst exhibits slightly higher catalytic activity than  $\delta$ -FeOOH in the heterogeneous solar photo-Fenton process but is less stable. The oxidation efficiency of basic blue 9 and acid green 50, analytical textile dyes, is compared to that of wastewater dye. The as-prepared catalysts are highly efficient for the wastewater treatment and the synthetic solutions prepared from the analytical textile dyes. High mineralization (over 90%) of the organic components of wastewater was achieved at 5 h of solar photo-Fenton treatment.

**Keywords:** FeOOH catalyst, Heterogeneous solar photo-Fenton, Real wastewater treatment, Textile dye wastewater

Wastewater effluents from the textile industry contain toxic and poisonous chemicals that affect the human health and the life in aquatic ecosystems. Aqueous dyes are difficult to discolor due to their complex structure and synthetic origin, which make them persistent and recalcitrant in the aquatic environments. The worldwide environmental regulations have become more stringent towards wastewater discharges demanding efficient and environmentally friendly treatment technologies. Advanced oxidation processes (AOP) are considered environmentally friendly, no waste generating technologies, and represent an alternative for dye wastewater treatment<sup>1-4</sup>. The chemical and photochemical methods of the AOP have in common the *in-situ* generation of hydroxyl radicals, which are powerful nonspecific oxidants of toxic and bio refractive wastewater contaminants<sup>5-8</sup>, producing CO<sub>2</sub>, water and mineral acids as end-products. The photo-Fenton reaction is an efficient photochemical AOP that can be carried out through the irradiation of the sunlight. The sunlight irradiation has been increasingly used to detoxify effluents contaminated with recalcitrant organic compounds by the solar photo-Fenton process<sup>9-12</sup>, therefore, it becomes extremely important to save energy and improve the performance of various aqueous degradation processes.

The Fenton reaction involves the combination of H<sub>2</sub>O<sub>2</sub> with iron ions (Fe<sup>2+</sup>/Fe<sup>3+</sup>) in mildly acidic conditions leading to the generation of active intermediates (OH<sup>•</sup>, OOH<sup>•</sup> and R<sup>•</sup>radicals) by the iron catalyzed decomposition of the hydrogen peroxide. It has also been proposed the formation of a highly reactive iron-oxo complex (the ferryl ion, FeO<sup>2+</sup>) as the oxidative intermediate in the homogeneous Fenton reaction<sup>13</sup>. In addition, the soluble ferric complex (Fe(OH)<sup>2+</sup>, at ~50% predominance) is formed with interactions between H<sub>2</sub>O<sub>2</sub> and Fe<sup>2+14,15</sup> that undergoes UV-photo reduction to generate OH<sup>•</sup> and Fe<sup>2+</sup> in the photo-Fenton reaction. The Fe(OH)<sup>2+</sup> ion absorbs light at wavelengths up to about 410 nm<sup>15</sup>. The solar photons can also increase the rate of hydroxyl radical formation by photoreactions of H<sub>2</sub>O<sub>2</sub> ( $\lambda \leq 360\text{nm}$ )<sup>16</sup> leading to the generation of OH<sup>•</sup> radicals.

When iron-containing solids are used, as in the heterogeneous Fenton reaction, adsorption of the H<sub>2</sub>O<sub>2</sub> molecule at the surface of the active sites ( $\equiv\text{Fe}^{\text{III}}$ ) has been suggested<sup>17,18</sup>. Hence, Fe<sup>3+</sup> is reduced with the generation of less oxidative HO<sub>2</sub><sup>•</sup> radicals, followed by Fe<sup>3+</sup> regeneration with the formation of OH<sup>•</sup> radicals, additional to the occurrence of similar reactions as in the homogeneous Fenton mechanism pathway.

Iron-based materials have been increasingly used in the catalytic oxidation of organic contaminants in wastewater in the heterogeneous Fenton and in the heterogeneous photo-Fenton reaction. Recently,  $\alpha$ -Fe<sub>2</sub>O<sub>3</sub>,  $\gamma$ -Fe<sub>2</sub>O<sub>3</sub>, Fe<sub>2</sub>O<sub>4</sub>, and  $\alpha$ -FeOOH,  $\gamma$ -FeOOH, and  $\delta$ -FeOOH composites have been used in the Fenton and photo-Fenton reaction<sup>19-25</sup>. Liu *et al.*,<sup>19</sup> incorporated graphene oxide (GO) into the  $\alpha$ -Fe<sub>2</sub>O<sub>3</sub> catalyst to degrade various organic pollutants in the photo-Fenton process under UV light within wider pH range such as 3 to 12. These authors reported that the incorporation of GO with  $\alpha$ -Fe<sub>2</sub>O<sub>3</sub> improved the catalytic efficiency and selectivity of  $\alpha$ -Fe<sub>2</sub>O<sub>3</sub> towards cationic organics and phenol like compounds. Jin and collaborators<sup>20</sup> reported an unprecedented Fenton activity of Cu doped Fe<sub>3</sub>O<sub>4</sub>@FeOOH attributed to the formation of oxygen vacancy from in situ Fe substitution by Cu rather than promoted Fe<sup>3+</sup>/Fe<sup>2+</sup> cycle at neutral and alkaline pH (3.2 to 9.0). Qian *et al.*,<sup>21</sup> remarked that the visible light, induced photo catalysis assisted heterogeneous Fenton-like process in the  $\alpha$ -FeOOH/Mesoporous carbon composite system, which improved the OH<sup>•</sup> production efficiency and Fe(III)/Fe(II) cycle that further activated the interfacial catalytic sites producing an extraordinary high degradation and mineralization efficiency of phenol. Ma and coworkers<sup>22</sup> developed a magnetic  $\alpha$ -FeOOH/ $\gamma$ -Fe<sub>2</sub>O<sub>3</sub> nanocomposite to degrade and mineralize tetracycline hydrochloride inside a wide pH range (3-10) in the photo-Fenton process under visible light. The magnetic catalyst exhibited high activity which was attributed to the way the H<sub>2</sub>O<sub>2</sub> was activated. These authors proposed that  $\gamma$ -Fe<sub>2</sub>O<sub>3</sub> captured the photo generated electrons in the conduction band of  $\alpha$ -FeOOH inhibiting the reaction between electrons and H<sub>2</sub>O<sub>2</sub>. The photo generated holes can directly oxidize the tetracycline hydrochloride or react with H<sub>2</sub>O<sub>2</sub> to produce O<sub>2</sub><sup>•-</sup>. Therefore, these authors concluded that the organic compound can be degraded by OH<sup>•</sup>, holes and O<sub>2</sub><sup>•-</sup>, and the formed intermediates can be further oxidized to carboxylic acids, CO<sub>2</sub> and H<sub>2</sub>O. Da Silva and coworkers<sup>23</sup> observed an improvement of the photocatalytic activity of  $\delta$ -FeOOH upon H<sub>2</sub>O<sub>2</sub> addition to rhodamine-B solution during the photo-Fenton degradation. This was attributed to the OH<sup>•</sup> formation by direct H<sub>2</sub>O oxidation or by H<sub>2</sub>O<sub>2</sub> reduction considering that the electron transfer from the conduction band of  $\delta$ -FeOOH to H<sub>2</sub>O<sub>2</sub> is thermodynamically favorable; additionally, the H<sub>2</sub>O<sub>2</sub>

retarded the electron-hole recombination in  $\delta$ -FeOOH increasing OH<sup>•</sup> formation. Other authors reported high degradation efficiencies with  $\gamma$ -FeOOH mixed with granular activated carbon to decolorize textile wastewater<sup>24</sup> and  $\alpha$ -FeOOH catalyst to degrade orange II dye in the photo-Fenton process<sup>25</sup>. In addition, Lima and collaborators<sup>26</sup> evaluated the photo catalytic activity of  $\delta$ -FeOOH/WO<sub>3</sub> nanocomposite during the degradation of rhodamine B dye (RhB) and indicated that RhB oxidation occurred through photocatalysis rather than the photosensitized process.

Du and collaborators<sup>27</sup> studied the photoinduced degradation of orange II in the presence of six different iron catalysts (like  $\alpha$ -Fe<sub>2</sub>O<sub>3</sub>,  $\gamma$ -Fe<sub>2</sub>O<sub>3</sub>, Fe<sub>2</sub>O<sub>4</sub>, and  $\alpha$ -FeOOH,  $\gamma$ -FeOOH, and  $\delta$ -FeOOH). These authors reported that dye photo degradation was enhanced with all catalyst in the presence of H<sub>2</sub>O<sub>2</sub>, AgNO<sub>3</sub> and NaF but the iron oxides appeared to be more active than the iron hydroxides. Pinto and collaborators<sup>18</sup> reported that  $\delta$ -FeOOH nanoparticles activated H<sub>2</sub>O<sub>2</sub> producing reactive radicals, which further promoted the oxidation of dye molecules. They also reported that the degradation rates depended on the amount of Fe<sup>2+</sup> generated *in situ* on the  $\delta$ -FeOOH surface.

This work is aimed at the discoloration and mineralization of the organic compounds present in the textile wastewater through the catalytic activity of iron oxyhydroxides ( $\delta$ -FeOOH and FeOOH) for the decomposition of hydrogen peroxide in the heterogeneous photo-Fenton reaction under solar irradiation. Iron-based materials are synthesized from ferrous and ferric salts using an easy and inexpensive procedure. The influence of important parameters that affects the degradation of the organic pollutants present in the wastewater is studied, such as initial concentration of H<sub>2</sub>O<sub>2</sub>, pH, catalyst load and initial chemical oxygen demand from the wastewater. In addition, a comparison of the degradation efficiency of analytical dyes with that of wastewater dye is observed.

## Experimental Section

### Chemicals

Sodium hydroxide (J. Baker), sulfuric acid (J. Baker), hydrogen peroxide (30%v/v, Meyer), ammonia ferrous sulphate (Meyer), and ferric ammoniacal sulphate (Alyt) were analytical grade and used as received. The industrial wastewater came from a local textile industry.

### Catalyst preparation

The synthesis of the iron oxyhydroxides catalyst ( $\delta$ -FeOOH) nanoparticles were prepared by mixing

100 mL of a solution containing 5.56g of ammonia ferrous sulphate ( $\text{Fe}(\text{NH}_4)_2(\text{SO}_4)_2 \cdot 6\text{H}_2\text{O}$ ) with 100 mL of a 2 M NaOH solution; a greenish rust precipitate was formed. An addition of 5 mL of 30%  $\text{H}_2\text{O}_2$  was followed with gently stirring, turning the precipitate to reddish brown (this is an evidence of the formation of  $\delta\text{-FeOOH}$ ) nanoparticles<sup>28</sup>. The precipitate was washed thrice with distilled water, dried at room temperature for four days, and placed in a vacuum desiccators at room temperature. The same procedure was carried out using the ferric ammoniacal sulphate ( $\text{FeNH}_4(\text{SO}_4)_2 \cdot 12\text{H}_2\text{O}$ ) to assess if the  $\delta\text{-FeOOH}$  was also formed and to evaluate the catalytic effect on the Fenton process for the wastewater. Thus, the catalyst formed from the ferric ion precursor is assigned here as FeOOH.

The morphology of produced materials was monitored with scanning electron microscopy (SEM) (Hitachi FE-SEM S-5500 integrated with an energy-dispersive X-ray spectrometer Bruker Quantax 200 for EDS elemental analysis); whereas powder X-ray diffraction (XRD) data were recorded by scanning  $2\theta$  in the range of  $20\text{--}70^\circ$ , with grazing incidence angle of  $0.5^\circ$  radiation in a Rigaku Geigerflex diffract meter (Cu-K $\alpha$ , Rigaku DMAX-2200).

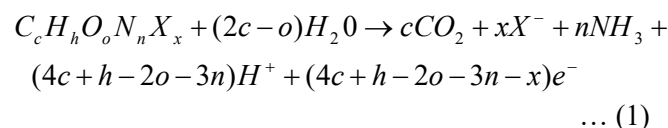
#### Wastewater treatment

Textile effluent, from a local industry inside the Yecapixtla Industrial Park in Morelos State, was collected, filtrated, acidified and used within the next five days. Table 1 depicts some physicochemical characteristics of such industrial effluent after filtration. A set of experiments were conducted in Pyrex reactors containing 250 mL of textile wastewater placed under the sunlight between 10h to 15h in sunny days.

The experiments were carried out to assess the performance of the as-prepared catalysts on the effluent treatment under several conditions, such as initial chemical oxygen demand (COD) of wastewater (52, 260 and 520  $\text{mgL}^{-1}$ ), pH (1.0, 3.0 and 7.0),  $\text{H}_2\text{O}_2$  concentration ( $1.7 \times 10^{-3}$ ,  $3.3 \times 10^{-3}$  and  $7.0 \times 10^{-3}$   $\text{mol L}^{-1}$ ),

and catalyst load (100, 300 and 500  $\text{mg L}^{-1}$ ). Samples were taken at pre-selected time intervals to measure the absorbance (at 570 nm), COD and total organic carbon (TOC). COD and TOC were analyzed using standard methods and standard reagents (HACH).

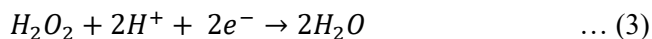
The overall oxidation process of an organic compound can be described by reaction (1):



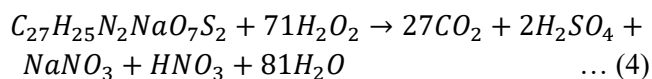
Where the atoms of carbon (C), hydrogen (H), oxygen (O), nitrogen (N) and halogen (X) have their respective number of atoms represented by  $c$ ,  $h$ ,  $o$ ,  $n$  and  $x$ . Therefore, the number of electrons involved in the oxidation process is  $(4c + h - 2o - 3n - x)$ ; clearly, each organic compound will contribute with different number of electrons. Nevertheless, the number of the organic compounds (dyes, stabilizers, additives, etc.) and their composition in the industrial effluent is unknown; thus, to know the initial amount of  $\text{H}_2\text{O}_2$  to oxidize the organic compounds present in the textile effluent, it is assumed that an equivalent COD of a known organic compound (i.e. acid green 50 dye with a condensed molecular formula:  $C_{27}H_{25}N_2NaO_7S_2$ ) may satisfy such demand. Thus, considering such analogy, the determination of the hydrogen peroxide concentration, based on the theoretical hypothesis for a complete mineralization of one mole of the acid green 50 (AG50), is given by:

$$[H_2O_2] = \frac{(4c+h-2o-3n-x)}{2} \quad \dots (2)$$

Where  $(4c + h - 2o - 3n - x)$  is the number of electrons of AG50 ( $C_{27}H_{25}N_2NaO_7S_2$ ), and the denominator comes from the number of electrons transferred from the  $\text{H}_2\text{O}_2$ :



Thus, 71 mol of  $\text{H}_2\text{O}_2$  is needed to oxidize one mole of AG50, as depicted in reaction (4),



Then, based on this reaction,  $3.3 \times 10^{-3}$  mol of  $\text{H}_2\text{O}_2$  would be required for a complete oxidation of AG50 dye solution with an initial COD content of 52  $\text{mgL}^{-1}$ . Thus, it is expected that  $3.3 \times 10^{-3}$   $\text{mol L}^{-1}$  of  $\text{H}_2\text{O}_2$  would be required to mineralize completely the organic compounds in the textile wastewater with an equivalent COD of 52  $\text{mgL}^{-1}$ .

Table 1—Characteristics of the industrial effluent after filtration

Parameters	Textile wastewater
Colour	Dark blue
pH	$7.71 \pm 0.02$
COD ( $\text{mgL}^{-1}$ )	$1275 \pm 1$
TOC ( $\text{mgL}^{-1}$ )	$520 \pm 0.5$
Total alkalinity ( $\text{mgL}^{-1}$ as $\text{CaCO}_3$ )	$65 \pm 0.07$
Total hardness ( $\text{mgL}^{-1}$ as $\text{CaCO}_3$ )	$9.7 \pm 0.05$

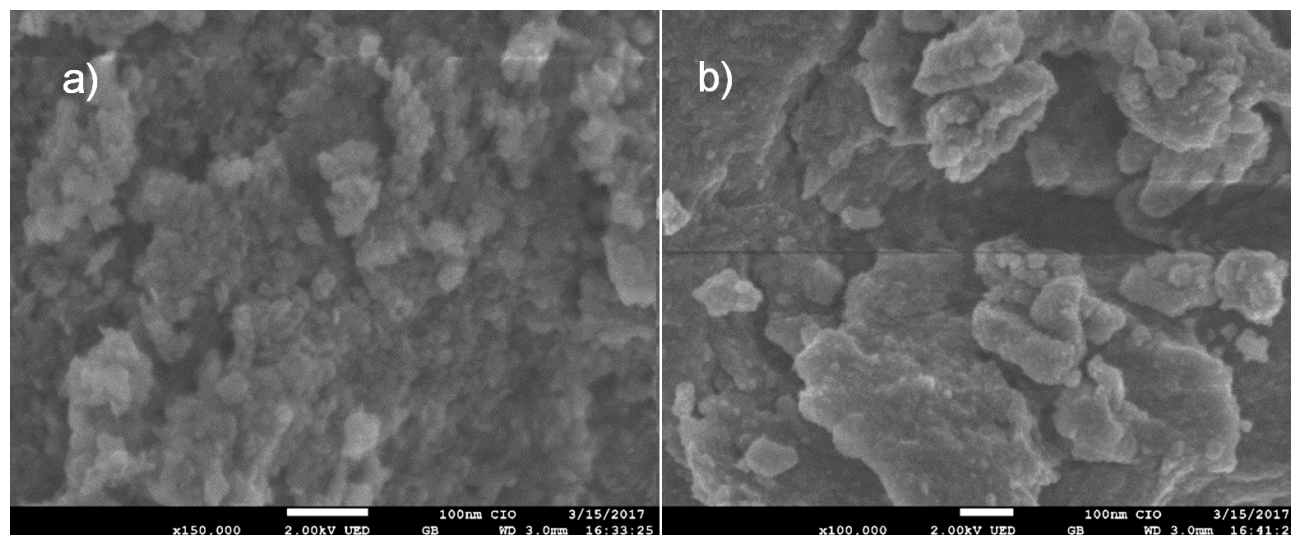


Fig. 1—SEM images of the a)  $\delta$ -FeOOH, and b) FeOOH.

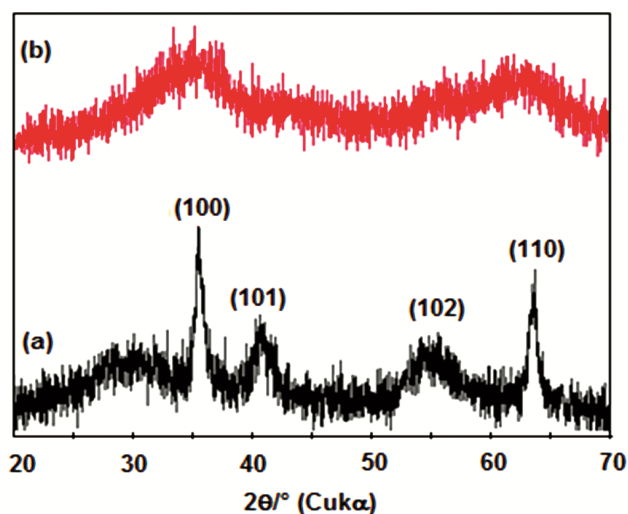


Fig. 2—Powder X-ray diffraction pattern of Fenton like-catalysts: a)  $\delta$ -FeOOH, and b) FeOOH.

## Results and Discussion

### Powder characterization

The morphology of the as-obtained catalysts is shown on the SEM images in Fig. 1, where porous structures with elongated and rounded aggregate particles are observed; such particles are formed with numerous small and uniform nanoparticles present in both images, although Fig. 1b (FeOOH) presents more nanoparticle agglomeration than the morphology of  $\delta$ -FeOOH powder (Fig. 1a). The XRD pattern, shown in Fig. 2a, presents a single phase corresponding to  $\delta$ -FeOOH, in agreement with other workers<sup>23,29</sup>. However, for the case of the FeOOH catalyst (Fig. 2b), some peaks of the X-ray diffraction pattern are not defined (absence of 101 and 102)

suggesting an amorphous structure because of the absence of peak periodicity, remaining those broad peaks of short range (100 and 110). Using the Scherrer equation, the mean crystallite dimension for the  $\delta$ -FeOOH is  $12.7 \pm 2$  nm.

### Heterogeneous solar photo-Fenton for the textile wastewater

The local textile effluent, due to its own nature, has a variable composition with different organic compounds and suspended solids which make more difficult its treatment. The oxidation of organic pollutants leads to the formation of intermediate species which can be further mineralized to  $\text{CO}_2$ ,  $\text{H}_2\text{O}$  and inorganic salts. Thus, the influence of parameters such as initial concentration of  $\text{H}_2\text{O}_2$ , solution  $\text{pH}$ , catalyst content, COD of the wastewater, reuse, stability and recovery of catalyst on the wastewater treatment are evaluated.

### Influence of $\text{H}_2\text{O}_2$ initial concentration

Colour measurements from the textile wastewater treated in the heterogeneous solar photo-Fenton process (Fig. 3a) show that an increase or decrease in the initial concentration of  $\text{H}_2\text{O}_2$ , with respect to the stoichiometric assumption ( $3.3 \times 10^{-3} \text{ mol L}^{-1}$ ), produced similar color removal at 5h ( $\sim 94\%$ ) using either  $\delta$ -FeOOH or FeOOH catalyst. Initially, faster color removal occurs within 3h for the stoichiometry using the FeOOH catalyst. This is attributed to the higher catalytic decomposition of the  $\text{H}_2\text{O}_2$  by the ion  $\text{Fe}^{3+}$  species on the FeOOH surface to produce  $\bullet\text{OH}$  radicals under the sunlight. In addition, competitive reactions between  $\text{H}_2\text{O}_2$  (in excess) and the  $\bullet\text{OH}$  radicals take place which leads to a discoloration decrease. The effect of the initial concentration of

$\text{H}_2\text{O}_2$  is notorious on the COD removal (Fig. 3b) for  $\delta\text{-FeOOH}$  or  $\text{FeOOH}$  catalyst. This is because the  $\text{H}_2\text{O}_2$  acts as a scavenger for hydroxyl radicals. The optimal initial concentration of  $\text{H}_2\text{O}_2$  is  $3.3 \times 10^{-3} \text{ mol L}^{-1}$  indicating that our approach was suitable to know the amount of  $\text{H}_2\text{O}_2$  required for oxidizing the unknown composition of the industrial textile wastewater effluent.

#### Treatment of the industrial textile wastewater under several processes

The discoloration of wastewater as a function of time for several experiments carried out in the catalysts in darkness ( $\delta\text{-FeOOH}$  and  $\text{FeOOH}$ ) and heterogeneous Fenton is depicted in Fig. 4a, whereas several processes such as photolysis, photolysis with Figure 4b shows wastewater discoloration under sunlight using  $\text{H}_2\text{O}_2$ , photolysis with catalysts and heterogeneous photo-Fenton. As can be seen, 5% of colour removal is reached at 5h by the sole presence of each catalyst in darkness. This is attributed to wastewater discoloration because of the adsorption

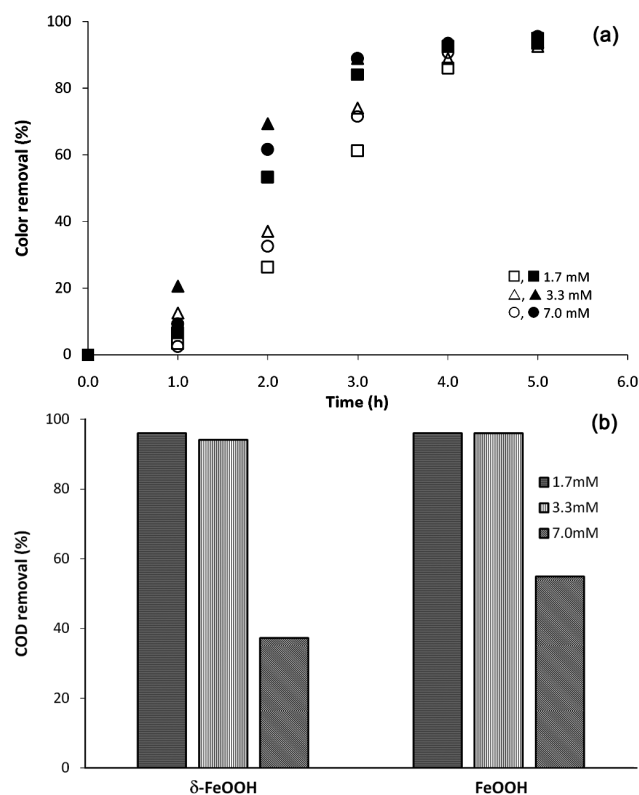


Fig. 3—Influence of the initial  $\text{H}_2\text{O}_2$  concentration on the colour abatement (a) and on COD removal (b) during the heterogeneous solar photo-Fenton process ( $52 \text{ mgL}^{-1}$  of initial COD of the wastewater, solution  $\text{pH}=1$ ,  $100 \text{ mgL}^{-1}$  catalyst load).  $\delta\text{-FeOOH}$  (open symbols) and  $\text{FeOOH}$  (solid symbols). The reported COD in Fig. 3b corresponds at 5h reaction time.

process taken place in the surface of the catalysts which exhibit similar adsorption capacity of the wastewater colour.

The treatment of wastewater by the heterogeneous Fenton increased the color removal to 20% and 32% at 5h using  $\delta\text{-FeOOH}$  and  $\text{FeOOH}$  catalysts, respectively. This is a result of the enhanced formation of radicals that were involved in the oxidation of the organic compounds present in the wastewater by the Fenton process. It is observed higher colour removal by the  $\text{FeOOH}$  catalyst, being attributed to the higher capacity of the active sites ( $\equiv\text{Fe}^{3+}$ ) on the catalyst surface to activate the  $\text{H}_2\text{O}_2$ , generating reactive species such as  $\bullet\text{OH}$  radicals and  $\text{O}_2\bullet^-$ . It has been suggested a competitive adsorption pathway between  $\text{H}_2\text{O}_2$  and the wastewater color, in which wastewater colour partly desorbs from the catalysts surface<sup>18</sup>. According to these authors, the  $\bullet\text{OH}$  radicals are responsible for the

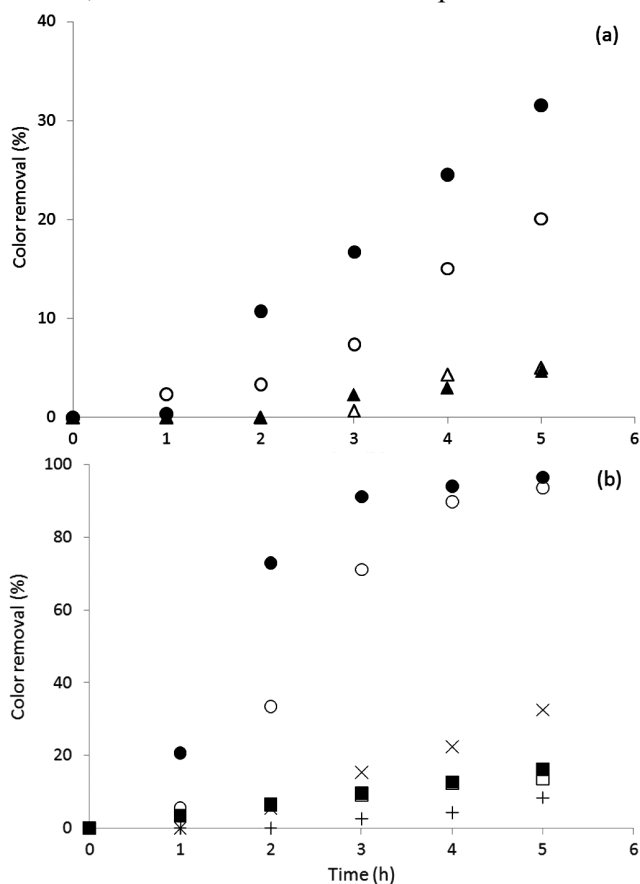


Fig. 4—Colour removal from the wastewater by (a) the catalysts in darkness ( $\triangle$ ,  $\blacktriangle$ ), heterogeneous Fenton ( $\circ$ ,  $\bullet$ ) and by (b) sunlight (+), sunlight (+)  $\text{H}_2\text{O}_2$  (x), sunlight + catalysts ( $\square$ ,  $\blacksquare$ ) and heterogeneous solar photo-Fenton ( $\circ$ ,  $\bullet$ ) using  $\delta\text{-FeOOH}$  (open symbols) and  $\text{FeOOH}$  (solid symbols) as catalysts ( $52 \text{ mgL}^{-1}$  of initial COD, solution  $\text{pH}=1$ ,  $100 \text{ mgL}^{-1}$  catalyst load and  $3.3 \times 10^{-3} \text{ molL}^{-1} \text{H}_2\text{O}_2$ ).

wastewater treatment due to the adsorption of  $\text{H}_2\text{O}_2$  on the catalyst surface ( $\equiv\text{Fe}^{3+}$ ). The adsorbed  $\text{H}_2\text{O}_2$  reacts with the active sites ( $\equiv\text{Fe}^{3+}$ ) of the catalyst surface forming  $\equiv\text{Fe}^{2+}$  and  $\text{O}_2\cdot^-$  radicals; the adsorbed  $\text{H}_2\text{O}_2$  also reacts with  $\equiv\text{Fe}^{2+}$  generated *in situ* to form highly active  $\cdot\text{OH}$  radicals and  $\equiv\text{Fe}^{3+}$ . Finally, the  $\cdot\text{OH}$  radicals attack the organic matter present in the textile wastewater producing oxidation by-products.

When the oxidation is carried out upon solar photolysis, solar photolysis with  $\text{H}_2\text{O}_2$ , solar photolysis with  $\delta\text{-FeOOH}$  and solar photolysis with  $\text{FeOOH}$ , about 9%, 33%, 14% and 16% color removal is obtained at 5h, respectively; in contrast with ~94% and ~97% color removal attained by the heterogeneous solar photo-Fenton reaction using  $\delta\text{-FeOOH}$  and  $\text{FeOOH}$ , as catalyst, respectively (Fig. 4b). Clearly, the solar light irradiation enhances the wastewater colour removal compared to the reactions taken place in darkness, regardless of the solar process used. Thus the sunlight highly enhances the  $\cdot\text{OH}$  radical production by the activation of the  $\text{H}_2\text{O}_2$  and the active sites of the surface of the catalysts ( $\delta\text{-FeOOH}$  and  $\text{FeOOH}$ ), that increases the catalytic activity for  $\text{H}_2\text{O}_2$  decomposition, leading to the highly increased wastewater colour removal in the heterogeneous solar photo-Fenton, with  $4.1\times 10^{-2}\text{h}^{-1}$  and  $4.8\times 10^{-2}\text{h}^{-1}$  rate constants for  $\delta\text{-FeOOH}$  and  $\text{FeOOH}$ , respectively (Table 2). The discoloration of the wastewater follows a pseudofirst order reaction during the oxidation of the organic compounds in the wastewater by these processes upon solar light irradiation (Table 2); the pseudo first order rate constants are estimated from the plot of  $\ln(\text{Abs}_0/\text{Abs})$  vs time. The highest wastewater discoloration by the heterogeneous solar photo-Fenton is explained by the combined effects of the UV-sunlight (~5% of the global solar irradiation) with  $\text{H}_2\text{O}_2$  and the visible sunlight with the  $\equiv\text{Fe}^{3+}$ , active sites, to produce hydroxyl radicals that attack the dye compounds in the wastewater. Finally, the solar photo

Table 2—Kinetic discoloration rates

Degradation process	k (h <sup>-1</sup> )	R <sup>2</sup>
Solar photolysis	0.026	0.9135
Solar photolysis with $\text{H}_2\text{O}_2$	0.068	0.9685
Solar photolysis with $\delta\text{-FeOOH}$	0.039	0.9359
Solar photolysis with $\text{FeOOH}$	0.038	0.9587
Heterogeneous solar photo-Fenton with $\delta\text{-FeOOH}$	0.412	0.9598
Heterogeneous solar photo-Fenton with $\text{FeOOH}$	0.482	0.9868

52 mgL<sup>-1</sup> COD contents of wastewater,  $3.3\times 10^{-3}\text{molL}^{-1}\text{H}_2\text{O}_2$ , 100 mgL<sup>-1</sup> catalyst load and pH 1

activation of the  $\text{H}_2\text{O}_2$  ( $6.8\times 10^{-2}\text{h}^{-1}$ ) is higher than the solar photoactivation of the active sites of the catalysts ( $3.9\times 10^{-2}\text{h}^{-1}$  and  $3.8\times 10^{-2}\text{h}^{-1}$  for  $\delta\text{-FeOOH}$  and  $\text{FeOOH}$ , respectively) which might be attributed to the homogeneity of the molecules of  $\text{H}_2\text{O}_2$  in the aqueous system that readily receives the sunlight.

#### Effect of initial solution pH

The pH in the aqueous system is an important parameter since it affects the catalytic performance and the stability of the catalysts. Figure 5 shows the influence of the initial solution pH (1, 3, 5 and 7) on color removal of the wastewater by the heterogeneous solar photo-Fenton process. It is found that the discoloration decreases with increasing the initial pH of the solution. The highest color removal is acquired using the catalysts at pH 1 and also at pH 3 for  $\text{FeOOH}$  catalyst. This is attributed to iron leaching from the catalyst surfaces at  $\text{pH}\leq 3$ , implying that both heterogeneous and homogeneous Fenton processes took place. The concentration of total iron in the bulk solution was measured at 5h of reaction and found that it decreased as the initial pH of the solution increased. The amount of total iron leached at 5h of reaction is 14.0 mgL<sup>-1</sup> and 7.7 mgL<sup>-1</sup> for  $\delta\text{-FeOOH}$  and  $\text{FeOOH}$  catalysts, respectively at pH 1; whereas at  $\text{pH}\geq 3$  iron leaching was less than 1.0 mgL<sup>-1</sup> at the same time of reaction.

#### Influence of catalyst content

Figure 6 shows the color or COD removal as function of catalyst content by the heterogeneous solar photo-Fenton using  $\delta\text{-FeOOH}$  and  $\text{FeOOH}$  catalysts in the wastewater, containing 52 mgL<sup>-1</sup> of initial COD,  $3.3\times 10^{-3}\text{molL}^{-1}\text{H}_2\text{O}_2$  and pH 1 at 5h reaction. By increasing the amount of catalyst used no

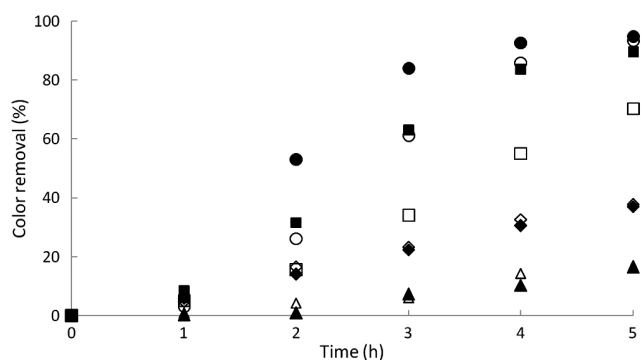


Fig. 5—Colour removal of the wastewater as function of pH by heterogeneous solar photo-Fenton using  $\delta\text{-FeOOH}$  (open symbols) and  $\text{FeOOH}$  (solid symbols) catalysts in wastewater containing 52 mgL<sup>-1</sup> of initial COD, 100 mgL<sup>-1</sup> catalyst load and  $3.3\times 10^{-3}\text{molL}^{-1}\text{H}_2\text{O}_2$ : (○, ●) pH 1, (□, ■) pH 3, (◇, ◆) pH 5 and (△, ▲) pH 7.

increase in the discoloration is observed for  $\delta$ -FOOH catalyst, but a slight decrease is shown as the content of FeOOH increases; similar trend is observed for COD abatement which decreases as catalyst content increases, in which the performance of the FeOOH is poor at catalyst load  $>100 \text{ mgL}^{-1}$ . As can be seen overloading of the catalysts ( $>100 \text{ mgL}^{-1}$ ) hinders COD removal of the textile wastewater. This is attributed to the high concentration of the catalysts that confers a high turbidity to the reactant solution, producing a screening effect for the sunlight penetration to catalytically decompose the  $\text{H}_2\text{O}_2$  in the Fenton reaction. This results in less  $\bullet\text{OH}$  radicals present in the reaction wastewater with the subsequent decrease in the COD removal.

Figure 7 depicts color removal as function of initial COD content by the heterogeneous solar photo-Fenton using  $\delta$ -FOOH and FeOOH catalysts in the wastewater, containing  $100 \text{ mgL}^{-1}$  of catalyst,  $3.3 \times 10^{-3} \text{ mol L}^{-1} \text{ H}_2\text{O}_2$  and  $\text{pH } 1$ . As can be seen, increasing the initial COD

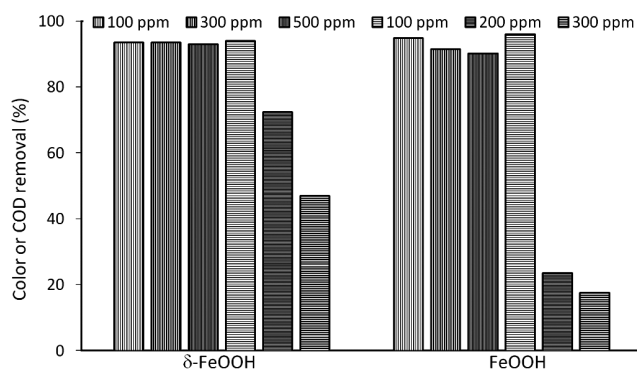


Fig. 6—Removal of colour (vertical line pattern) or COD (horizontal line pattern) from the wastewater as function of catalyst content by heterogeneous solar photo-Fenton at 5h reaction.

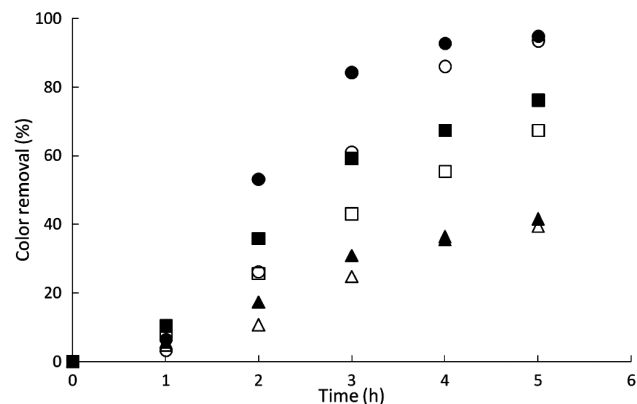


Fig. 7—Colour removal as function of different initial COD of wastewater by heterogeneous solar photo-Fenton using  $\delta$ -FOOH (open symbols) and FOOH (solid symbols) catalysts; initial COD in  $\text{mgL}^{-1}$ : ( $\circ$ ,  $\bullet$ ) 52, ( $\square$ ,  $\blacksquare$ ) 260 and ( $\triangle$ ,  $\blacktriangle$ ) 520.

content, a decrease in the rate of discoloration is observed. These phenomena may be explained by (i) higher initial concentration of  $\text{H}_2\text{O}_2$  are required by the stoichiometry to abate higher COD contents<sup>3</sup>, and (ii) the number of active sites available is decreased by the dye molecules because of their competitive adsorption on the surface of the catalysts<sup>30</sup>.

Since the hydrogen peroxide is photolyzed by the sunlight to form  $\text{OH}\bullet$  reactive species, it is expected that its initial concentration would be consumed faster than in darkness, as observed by other authors<sup>12,31</sup>.

Thus, to obtain higher discoloration of the wastewater dye (over 90%) an attempt was carried out using reaction times  $\geq 5\text{h}$  with additions of  $\text{H}_2\text{O}_2$  every 2.5h (Fig. 8). As can be seen in this figure, the rate of discoloration is enhanced, with respect to that reported in Fig. 7, by the hydrogen peroxide addition in the experiments using initial COD content of 52 and 260  $\text{mgL}^{-1}$ , but for 520  $\text{mgL}^{-1}$  such enhancement is not observed due to a decreased in the sunlight intensity by a cloudy period of about 3h, as shown in this figure. Such enhancement is explained by the increased amount of  $\text{OH}\bullet$  species provided by the fresh additions of  $\text{H}_2\text{O}_2$  that were (i) catalytically decomposed by the active sites of the catalysts surface and (ii) by the continuous solar photo activation of the  $\text{H}_2\text{O}_2$  and the active species on the catalyst surface. Finally, wastewater treatment not only involves color removal but also mineralization of both the dye molecules and the byproducts generated during the reaction time. Thus,  $\text{H}_2\text{O}_2$  additions promoted over 90% mineralization of the organic components present in the wastewater, as depicted in Table 3. It is possible that

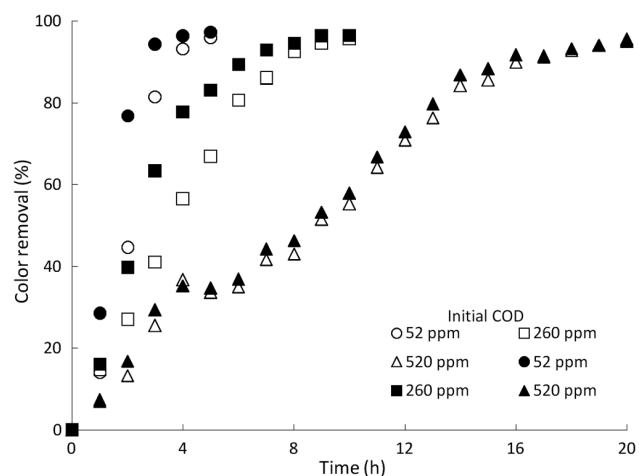


Fig. 8—Colour removal vs initial COD of wastewater by heterogeneous solar photo-Fenton using  $\delta$ -FOOH (open symbols) and FOOH (solid symbols) catalysts with  $\text{H}_2\text{O}_2$  additions every 2.5h



total mineralization was not acquired due to the presence of other species (such as additives, color stabilizers, etc.) in the textile wastewater.

#### Reuse, stability and recovery of catalyst

The reuse, stability and recovery of the catalyst represent a key issue regarding to the industrial potential application. When the catalyst is used as suspended powdered particles, a filtration step is required to recover the catalyst from the reaction medium. Therefore, the development of magnetic catalysts provides an easy, fast and inexpensive separation upon the application of a magnetic field which simplifies its recovery and reusability<sup>18,32</sup>. The reusability and stability of the catalysts after successive recycling during the heterogeneous solar photo-Fenton process are shown in Fig. 9. It is observed that the discoloration efficiency rapidly decreases for the FeOOH catalyst in the second cycle and for the  $\delta$ -FeOOH in the third cycle. The reduction in the catalyst efficiency may be caused by iron leaching from the surface of the catalysts and loss of catalyst through filtration (for catalyst recycling). The active sites of the  $\delta$ -FeOOH catalyst exhibits good activity and reusability up to two successive cycles, but the other catalyst exhibits poor recyclability because the iron leaches in higher extend than in the former catalyst. Thus, leaching of iron is indicative of the instability of the catalysts and so an elimination step from the effluent is required.

#### Treatment of the textile wastewater compared with artificial dye solutions

The performance of the as-prepared iron catalysts in the degradation of two analytical textil dyes, by the heterogeneous solar photo-Fenton process, was observed and compared with the textile wastewater discoloration. Thus, basic blue 9 ( $C_{16}H_{18}N_3SCl$ ) and acid green 50 ( $C_{27}H_{25}N_2NaO_7S_2$ ) dyes (provided by the local textile industry) were chosen. The amount of  $H_2O_2$  that corresponds to the stoichiometry for acid green 50 (AG50), and basic blue 9 (BB9) was used. The molecule of AG50 contains additional atoms of sodium and oxygen while BB9 contains chloride atoms, the rest of the atoms is common in both molecule dyes. Therefore, the oxidation of BB9 needs less amount of  $H_2O_2$  than the AG50, since  $102e^-$  and  $142e^-$  are needed to be withdrawn from BB9 and AG50, respectively.

Thus, two artificial dye solutions containing  $52\text{ mgL}^{-1}$  of initial COD were prepared, one with BB9 and the other with AG50, and then were subjected to

the oxidation by the heterogeneous solar photo-Fenton using  $\delta$ -FOOH and FOOH catalysts, as depicted in Fig. 10. As can be seen, the discoloration of the textile wastewater gradually increases until about 95% of color removal is obtained at 5h with both catalysts. The color removal for the BB9 solution using  $\delta$ -FeOOH and FeOOH catalysts is about 94% and 96% at 1.5h (increasing to 96% and 98% at 2.5h), respectively. Whereas about 87% of discoloration is attained for the AG50 dye solution with both catalysts at the same reaction time of 1.5h. Clearly, higher color removal is attained at shorter reaction times for the analytical dye solutions than that for the textile wastewater. This is attributed to the greater burden of other organic compounds contained in textile wastewater which makes treatment difficult. Nevertheless, it was possible to get a high degree of mineralization (>90%) of the

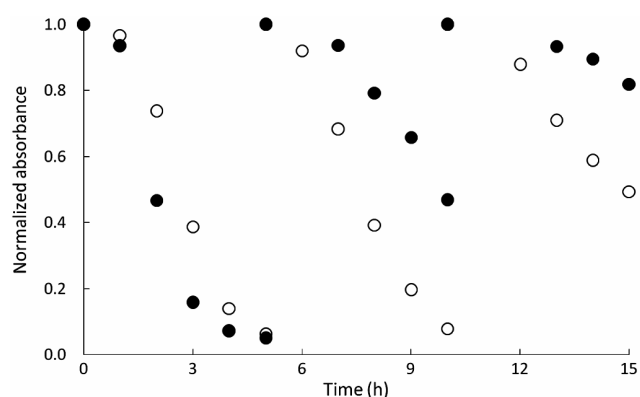


Fig. 9—Absorbance decrease vs catalyst cycling during dye wastewater treatment by heterogeneous solar photo-Fenton using  $\delta$ -FOOH (open symbols) and FOOH (solid symbols).  $52\text{ mgL}^{-1}$  of initial COD,  $100\text{ mgL}^{-1}$  catalyst load and  $3.3 \times 10^{-3}\text{ molL}^{-1}$   $H_2O_2$  at pH 1.

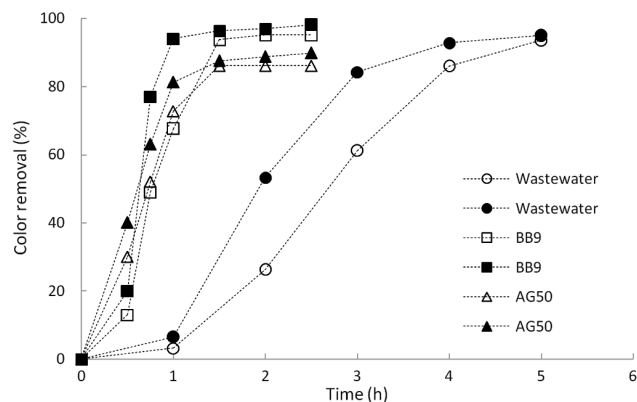


Fig. 10.—Colour removal from wastewater, basic blue 9 (BB9) and acid green 50 (AG50) dyes vs time by heterogeneous solar photo-Fenton ( $52\text{ mgL}^{-1}$  of initial COD of each dye solution,  $100\text{ mgL}^{-1}$  catalyst and  $3.3 \times 10^{-3}\text{ molL}^{-1}$   $H_2O_2$  at pH 1).



Table 3—Removal of total organic carbon (TOC) from different initial COD content in the textile wastewater by the heterogeneous solar photo-Fenton

DQO (mgL <sup>-1</sup> )	$\delta$ -FeOOH catalyst	FeOOH catalyst	Time (h)
	TOC (%)	TOC (%)	
52	96	97	5
260	92	94	10
520	95	96	20

organic components present in the textile wastewater at 5 h, as shown in Table 3.

### Conclusion

Successful discoloration and mineralization of the organic compounds present in the textile wastewater was achieved through the catalytic activity of iron oxyhydroxides in the heterogeneous solar photo-Fenton reaction. The amorphous FeOOH catalyst exhibited slightly higher catalytic activity than  $\delta$ -FeOOH in the heterogeneous solar photo-Fenton process but it was less stable. The as-prepared catalysts are highly efficient for the mineralization of the organic pollutants contained in the wastewater and the solutions prepared from the analytical dyes. The oxidation of basic blue 9 and acid green 50 was faster than that of organic compounds present in textile wastewater. High mineralization (over 90%) of the organic compounds present in the textile wastewater was achieved at 5 h.

### Acknowledgements

The authors would like to thank CONACYT for the grant given to Karen E. Barrera-Salgado. We are also grateful to CONACYT because this work was partially supported by the project of Problemas Nacionales 2015-01-1651: “Diseño y Construcción de Potabilizador Integral Solar de Agua para Comunidades Rurales”.

### References

- Martínez-Huitle C A & Brillas E, *Appl Catal B Environ*, 87 (2009) 105.
- Martínez S S & Uribe E V, *Ultrason Sonochem*, 19 (2012) 174.
- Ramos Preza, *Desalin Water Treat*, 52 (2014) 3526.
- Figueroa S, Vázquez L & Alvarez-Gallegos A, *Water Res*, 43 (2009) 283.
- Martínez S S & Bahena C L, *Water Res*, 43 (2009) 33.
- Pignatello J J, Oliveros E & MacKay A, *Crit Rev Environ Sci Technol*, 36 (2006) 1.
- Sirés I & Brillas E, A Review *Environ Int*, 40 (2012) 212.
- Alvarez-Gallegos A & Pletcher D, *Electrochim Acta*, 44 (1998) 853.
- Klamerth N, *Water Res*, 44 (2010) 545.
- Trovó A G, *Water Res*, 43 (2009) 3922.
- Malato S, *Catal Today*, 76 (2002) 209.
- Pineda Arellano C A, González A J, Martínez S S, Salgado-Tránsito I & Franco C P, *J. Photochem. Photobiol. A Chem*, 272 (2013) 21.
- Kremer M L, *Phys Chem Chem Phys*, 1 (1999) 3595.
- Boye B, Brillas E & Dieng M M, *Electrochim Acta*, 540 (2003) 25.
- Huston P L & Pignatello J J, *Water Res*, 33 (1999) 1238.
- Pignatello J J, Liu D & Huston P, *Environ Sci Technol*, 33 (1999) 1832.
- Dantas T L P, Mendonça V P, José H J, Rodrigues A E & Moreira R F P M, *Chem Eng J*, 118 (2006) 77.
- Pinto I S X, *Appl Catal B Environ*, 119 (2012) 175.
- Liu Y, Jin W, Zhao Y, Zhang G & Zhang W, *Appl Catal B Environ*, 206 (2017) 642.
- Jin H, *Environ Sci Technol*, 51 (2017) 12699.
- Qian X, *Environ Sci Technol*, 51 (2017) 3993.
- Ma Y, Wang B, Wang Q & Xing S, *Chem Eng J*, 354 (2018) 1.
- da Silva A, *J Photochem Photobiol A Chem*, 332 (2017) 54.
- Sheydaei M, Aber S & Khataee A, *J Mol Catal A Chem*, 392 (2014) 229.
- Miao X, Dai H, Chen J & Zhu J, *Sep Purif Technol*, 200 (2018) 36.
- Lima LV C, *Appl Catal B Environ*, 165 (2015) 579.
- Du W, Xu Y & Wang Y, *Langmuir*, 24 (2008) 175.
- Perng L H, Tung I C & Chin T S, *Le J Phys*, 7 (1997) 519.
- Chagas P, *J Nanoparticle Res*, 15 (2013).
- Azabou S, Najjar W, Gargoubi A, Ghorbel A & Sayadi S, *Appl Catal B Environ*, 77 (2007) 166.
- Vergara-Sánchez J & Silva-Martínez S, *Water Sci Technol*, 62 (2010) 77.
- Koch C B, *Phys Chem Miner*, 22 (1995) 333.